[6] Bauman Moscow State Technical University, Moscow, Baumanskaya 2-ya, 5, 105005, Russia e-mail: sv_ryzhov@mail.ru

Millimeter and X-ray emission from the 5 July 2012 solar flare
Solar Physics

Yu.T. Tsap[1,2] · **V.V. Smirnova**[2,3,4] ·
G.G. Motorina[2] · **A.S. Morgachev**[2,5] ·
S.A. Kuznetsov[2,5] · **V.G. Nagnibeda**[3] ·
V.S. Ryzhov[6]

Abstract The 5 July 2012 solar flare (11:39 - 11:49 UT) with a growing millimeter spectrum between 93 and 140 GHz is considered. We use space and ground-based observations in X-ray, extreme ultraviolet, microwave, and millimeter wave ranges obtained with the Reuven Ramaty High-Energy Solar Spectroscopic Imager, Solar Dynamic Observatory (SDO), Geostationary Operational Environmental Satellite, Radio Solar Telescope Network, and Bauman Moscow State Technical University millimeter radio telescope RT-7.5. The main parameters of thermal and accelerated electrons were determined through the X-ray spectral fitting assuming the homogeneous thermal source and thick target model. From the data of the Atmospheric Imaging Assembly (SDO) and differential emission measure calculations is shown that the thermal coronal plasma gives a negligible contribution to the millimeter flare emission. Model calculations suggest that the observed growth of millimeter spectral flux with frequency **is determined by** gyrosynchrotron emission of high energy ($\gtrsim 300$ keV) electrons in the chromosphere. Consequences of the obtained results are discussed in the light of the flare energy release mechanisms.

Keywords: Flares, Energetic Particles; Radio Bursts, Association with Flares; X-Ray Bursts

[1] Crimean Astrophysical Observatory, Nauchny, Crimea,
298409 e-mail: yur_crao@mail.ru
[2] Pulkovo Observatory, Pulkovskoe Shaussee 65/1, St.
Petersburg, 196140 Russia e-mail: g.motorina@gao.spb.ru
[3] Sobolev Astronomical Institute, Saint Petersburg State
University, Universitetsky Pr.28, St.Petersburg, Petergof,
198504, Russia e-mail: vnagnibeda@gmail.com
4 University of Turku, Turku, FI20014 Finland e-mail:
vvsvid.smirnova@yandex.ru
[5] Radiophysical Research Institute of Lobachevsky
University, Nizhny Novgorod, Bolshaya Pecherskaya 25/12a,
603950, Russia e-mail:
a.s.morgachev@mail.ru, kuznetsov.sergey.a@yandex.ru

1. Introduction

The relation between thermal and non-thermal processes responsible for the flare plasma heating and particle acceleration is **rather debatable**. In this connection, observations in the sub-THz frequency range of $10^2 - 10^3$ GHz $(0.3 - 3.0$ mm$)$ can be very useful since they allow us to receive important information about thermal and high energy electrons (Raulin *et al.*, 1999; Lüthi *et al.*, 2004; Giménez de Castro *et al.*, 2009; Fleishman and Kontar, 2010; Trottet *et al.*, 2011; Krucker *et al.*, 2013) but the origin of sub-THz emission is still unclear (Fleishman and Kontar, 2010; Krucker *et al.*, 2013; Zaitsev *et al.*, 2013). In particular, spectral flux, which increases with frequency (positive spectral slope) between 200 and 400 GHz has been recently revealed during impulsive and gradual phases of some solar flares (Trottet *et al.*, 2002; Lüthi *et al.*, 2004; Kaufmann *et al.*, 2004; Silva *et al.*, 2007; Kaufmann *et al.*, 2009; **Fernandes** *et al.*, 2017). This contradicts the hypotheses about the gyrosynchrotron origin of sub-THz emission **from a quasi-homogeneous source** generated by the relativistic tail of non-thermal accelerated electrons (Trottet *et al.*, 2002; Raulin *et al.*, 2004; Lüthi *et al.*, 2004; Giménez de Castro *et al.*, 2009) and, hence, needs further investigations.

The sub-THz emission at the frequencies $\nu = 200 - 400$ GHz is currently **attributed** to the gyrosynchrotron emission of compact sources (Kaufmann *et al.*, 1986; Kaufmann and Raulin, 2006; Silva *et al.*, 2007; Trottet *et al.*, 2008), Cherenkov emission (Fleishman and Kontar, 2010), thermal bremsstrahlung emission (Lüthi *et al.*, 2004; Trottet *et al.*, 2008; Trottet *et al.*, 2011; Tsap *et al.*, 2016), and plasma mechanism (Sakai and Nagasushi, 2007; Zaitsev *et al.*, 2013). But models listed above have different disadvantages (Zaitsev *et al.*, 2013; Krucker *et al.*, 2013). In particular, the thermal mechanism implies large areas of emission sources (Lüthi *et al.*, 2004; Silva *et al.*, 2007; Trottet *et al.*, 2008; Trottet *et al.*, 2011; Tsap *et al.*, 2016) while gyrosynchrotron one requires the strong magnetic field B that exceeds a few thousand gauss (Silva *et al.*, 2007).

According to observations with the patrol telescopes at the Solar Radio Observatory of the University of Bern at 19 and 35 GHz of 115 events (1984-1992) with the spectral flux > 100 s.f.u., about 50% of bursts had the flat spectrum while 25% were characterized by the positive spectral slope (Correia *et al.*, 1994). These and other results (Akabane *et al.*, 1973; Chertok *et al.*, 1995) suggest that the positive spectral slope observed in the frequency range of $30 - 100$ GHz does not require special emission mechanisms. Consequently, solar flare observations with the Bauman Moscow State Technical University millimeter radio telescope RT-7.5 at 93 and 140 GHz can be very helpful.

It is well established that non-thermal gyrosynchrotron emission at radio wavelengths and bremsstrahlung hard X-rays from solar flares show very similar temporal behavior (White *et al.*, 2011). This suggests the common origin and evolution of accelerated electrons responsible for these two emissions. Since the bremsstrahlung emission mechanism **suggests fewer free parameters** than gyrosynchrotron one, X-ray observations allow us to get more reliable information about energetic electrons.

The aim of this work is to consider peculiarities of millimeter emission from the 5 July 2012 solar flare based on extreme ultraviolet (EUV) and X-ray observations. Section 2 presents instruments and observations. Section 3 is devoted to the interpretation of X-ray and millimeter emissions. The conclusions and discussions are given in Section 4.

2. Observations and data analysis

Millimeter observations were carried out with the radio telescope RT-7.5 (Rozanov, 1981; Smirnova *et al.*, 2013). This single-dish antenna of the Cassegrain type with a diameter of 7.75 meters is used for simultaneous observations at two frequencies 93 GHz (3.2 mm) and 140 GHz (2.2 mm). The half-power beam widths of the antenna are 1.5 and 2.5$'$ at 140 and 93 GHz, respectively. Two super-heterodyne receivers are included into the quasi-optical scheme, i.e., beams are overlapped to observe one chosen area on the solar disk **with an accuracy of about 1%**. The time constant that is equal to 1 s provides the sensitivity of receivers of about 0.3 K. Peculiarities of the antenna calibration and observational methods were described in detail by Tsap *et al.* (2016). **Note that the sky was clear during the flare observations on 5 July 2012. The atmospheric opacities for 93 GHz and 140 GHz at that time were equal to 0.22 and 0.54 Np, respectively. The corresponding uncertainties in the determination of the flare maximum flux densities were about 10 and 15%.**
Microwave (centimeter) measurements were performed with the Radio Solar Telescope Network (RSTN, San Vito) at 4.9, 8.8, and 15.4 GHz with time resolution of about 1 s (Guidice *et al.*, 1981). Additionally we used EUV and X-ray data obtained with the Solar Dynamic Observatory (SDO, Lemen *et al.*, 2012), Reuven Ramaty High-Energy Solar Spectroscopic Imager (RHESSI, Lin *et al.*, 2002), and Geostationary Operational Environmental Satellite (GOES, White *et al.*, 2005).
NOAA 1515 appeared at the south-eastern solar limb on 27 June 2012. The sunspot group was quite complex ($\beta\gamma\delta$ magnetic configuration) and had interesting dynamics. The images obtained with the Helioseismic and Magnetic Imager (SDO/HMI, http://sdo.gsfc.nasa.gov) on 1 and 2 July showed the splitting of the main spot for less than 24 hours. Over the next two days, the split-off sunspot moved towards and into the middle portion of the sunspot group. **This inevitably resulted in 5 high energetic (M5 or stronger) flares during its transit.** In particular, NOAA 1515 produced 9 M-flares on 5 July 2012. The most powerful flare M6.1 (S22E68) peaked in GOES X-rays at 11:44 UT. **This event had not pronounced impulsive phase (Figure 1) and was accompanied by the coronal mass ejection.** Radio and hard X-ray time profiles near the emission peak consisted of **similar** $10-20$ s pulsations. The most interesting feature is related to the unusual positive spectral slope of millimeter emission between 93 and 140 GHz (Figure 2). Note that the second peak (11:46:49 UT) of soft X-ray light curve (0.5-4 Å) coincides with the second temperature peak (Figure 3). **Using the SDO/HMI data, the strength of the magnetic field B in the region of energy release was estimated: $B \lesssim 2~kG$.**

3. X-ray analysis and millimeter emission mechanisms

Let us consider some possible non-thermal and thermal mechanisms of millimeter emission based on EUV and X-ray data obtained with the RHESSI and SDO satellites.

3.1. Non-thermal component

To estimate the coronal plasma parameters from the RHESSI X-ray observations we used an object-oriented program known as the Object Spectral Executive (OSPEX) (Schwartz *et al.*, 2002). The X-ray background-subtracted spectrum **for the time interval 11:44:16-11:44:28 UT** was fitted with the isothermal model (*f_vth.pro*) and collisional thick target model (*f_thick2.pro*) for energies 7-155 keV (Figure 4). The obtained parameters of the fit are: emission measure $EM = 1.17 \times 10^{49}$ cm^{-3}, plasma temperature $T = 24.25$ MK, low energy cutoff in the spectrum of accelerated electrons $E_l = 21.88$ keV, total integrated electron flux $F_e = 2.22 \times 10^{35}$ s^{-1}, and spectral index **of the electron density** $\delta_l = 4.75$. **It is worthy of note that the** *f_thick2.pro* **model gives the spectral index of electron flux** $\delta_b = \delta_l - 0.5$ **(G. Holman, personal communication). According the RHESSI PIXON 25-50 keV image (Hurford** *et al.***, 2002), the 50% contours of two hard X-ray sources correspond to the area** $S_X = 2.5 \times 10^{17}$ **cm**^{2} **(Figure 5).**

The observed similarity of hard X-ray and radio time profiles (Figure 1) shows evidence in favor of the common population of low ($\lesssim 300$ keV) and high ($\gtrsim 300$ keV) energy electrons responsible for emission (White *et al.*, 2011). This assumption agrees well with a lack of correlation of these profiles with the second temperature peak (Figure 3).

Spectral indices of low and high energy electrons can be different in the flare energy release region (e.g., Kundu *et al.*, 1994; Ramaty *et al.*, 1994; Hildebrandt *et al.*, 1998; Trottet *et al.*, 1998; Giménez de Castro *et al.*, 2009). Let's try to find the relation between corresponding number densities suggesting a broken power-law spectrum.

The integral flux of low energy electrons responsible for hard X-ray emission can be represented as follows

$$F_e = S_X \int_{E_l}^{E_b} v n_l(E) dE, \qquad (1)$$

where E_b is the break energy in the spectrum.

In turn, assuming the spectral density

$$n_l(E) = n_{0l} E^{-\delta_l}, \qquad (2)$$

where n_{0l} is the normalized coefficient, the number density of accelerated electrons can be estimated as

$$n_l = \int_{E_l}^{E_b} n(E) dE = \frac{n_{0l}}{\delta_l - 1} (E_l^{1-\delta_l} - E_b^{1-\delta_l}). \qquad (3)$$

For the non-relativistic particles we can adopt

$$v = \sqrt{\frac{2E}{\alpha m}}, \tag{4}$$

where the coefficient α=1-3 characterizes a degree of electron anisotropy. Thus, Equations (1-4) at $(E_b/E_l)^{\delta_l-1} \gg 1$ give

$$F_e = S_X \sqrt{\frac{2}{\alpha m}} n_{0l} \frac{E_l^{-\delta_l+3/2}}{\delta_l - 3/2} = \frac{\delta_l - 1}{\delta_l - 3/2} n_l v_l S_X,$$

i.e., the number density of low energy electrons

$$n_l = \frac{\delta_l - 3/2}{\delta_l - 1} \frac{F_e}{v_l S_X}, \tag{5}$$

where $v_l = \sqrt{2E_l/(\alpha m)}$.

Supposing that the spectral density of high energy electrons with $E \geqslant E_b$ is

$$n_h(E) = n_{0h} E^{-\delta_h},$$

where n_{0h} is the normalized coefficient, excluding the jump at the point E_b, $n_l(E_b) = n_h(E_b)$, the relationship between number densities of electrons takes the form (Tsap *et al.*, 2016)

$$n_h = \frac{\delta_l - 1}{\delta_h - 1} \left(\frac{E_l}{E_b} \right)^{\delta_l-1} n_l. \tag{6}$$

Thus, the number density of high energy electrons n_h depends on the relationship E_l/E_b and the spectral index δ_l while the dependence on δ_h is quite weak.

From Equations (5) and (6) we find

$$n_h \approx \frac{F_e}{\sqrt{2E_l/(\alpha m)} S_X} \frac{\delta_l - 1}{\delta_h - 1} \left(\frac{E_l}{E_b} \right)^{\delta_l-1}. \tag{7}$$

Using results of the X-ray spectral fitting, adopting $\alpha = 3$ (isotropic distribution), Equation (7) can be reduced to the following formula

$$n_h \approx 10^6 \frac{\delta_l - 1}{\delta_h - 1} \left(\frac{E_b}{100 \text{ keV}} \right)^{1-\delta_l} \text{ [cm}^{-3}]. \tag{8}$$

Equation (8) suggests that we can estimate the number density of high energy electrons n_h for the given values of the break energy E_b.

In terms of peculiarities of time profiles we can suppose that the observed millimeter emission is determined by the non-thermal gyrosynchrotron mechanism. However, as we have mentioned above the magnetic field should be rather strong ($B \gtrsim 1$ kG) in this case, i.e., the generation of millimeter emission should occur in the transition region and/or in the chromosphere, where

the magnetic field can achieve kilogauss values (Akhmedov *et al.*, 1982). The positive spectral slope can be caused by the absorption of low frequency radio emission in the **surrounding** quite cold and dense plasma (see also Ramaty and Petrosian, 1972). Indeed, the coefficient of the **free-free** absorption **is** $\eta_\nu \propto n_e^2/(\nu^2 T^{3/2})$, where n_e is the number density of thermal electrons (Zheleznyakov, 1970), therefore the centimeter radio emission can be suppressed at the flare loop footpoints.

It should be stressed that millimeter gyrosynchrotron emission is determined by high energy electrons with $E \gtrsim 1$ MeV (White and Kundu, 1992). **As a result, the peculiarities of this emission do not strongly depend on the values of the break energy E_b which can be varied in the range $100-500$ keV. For the break energy $E_b = 300$ keV** (Hildebrandt *et al.*, 1998) **and the spectral index $\delta_l = 4.75$ Equation (8) gives the number density of high energy electrons $n_h \approx 10^5/(\delta_h - 1)$ cm^{-3}. Then using the corrected version (A. Kuznetsov, personal communication) of fast GS code (https://sites.google. com/site/fgscodes/transfer)** proposed by Fleishman and Kuznetsov **(2010) and assuming that the source area $S_{GS} = S_X = 2.5 \times 10^{17}$ cm^2, we can calculate the spectrum for different combinations of geometrical depth $l = 4 \times 10^6 - 10^8$ cm, magnetic field $B = 50 - 1500$ G, spectral index $\delta_h = 2 - 7$, number densities $n_e = 10^{10} - 10^{12}$ cm^{-3} and temperatures $T = 0.6 \times 10^4 - 3 \times 10^5$ K of background plasma, and angles between the magnetic field and line-of-sight $\theta = 0 - 90°$. As a result, we found that a quite good agreement between observed and model millimeter spectrum can be achieved at $\delta_h = 2 - 2.6$, $l = 2.8 \times 10^7 - 10^8$ cm. The number density n_e changes from 5.5×10^{10} to 10^{12} cm^{-3} if the plasma temperature increases from 10^4 to 3×10^5 K. The magnetic field B and viewing angle θ can take values from 450 to 1500 G and $25 - 90°$, respectively, depending on a spectral index δ_h and the geometrical depth l.**

Figure 6 shows the example of numerical calculations for the source area in the chromosphere $S_{GS} = 2.5 \times 10^{17}$ cm^2, spectral index of non-thermal electrons $\delta_h = 2.1$, geometrical depth $l = 4.6 \times 10^7$ cm, magnetic field $B = 1380$ kG, plasma temperature $T = 0.1$ MK, number density of thermal electrons $n_e = 3.8 \times 10^{11}$ cm^{-3}, and line-of-sight $\theta = 70°$. The adopting parameters agree well with X-ray observations and correspond to the height of $1000 - 1500$ km where $n_e = 10^{11} - 10^{12}$ cm^{-3} and the degree of plasma ionization changes from 0.1 to 1 (Machado *et al.*, 1980; Qu and Xu, 2002). Note that we did not take into account the contribution of neutral atoms to the bremsstrahlung absorption η_ν since it is negligible (Zheleznyakov, 1970).

It should be stressed that (Zaitsev *et al.*, 2013) proposed that the plasma mechanism can be responsible for the sub-THz emission in the solar chromosphere. Let us consider this possibility for our event in more detail.

The condition of the Langmuir wave excitation by electron beam can be represented as (Zaitsev *et al.*, 2013)

$$\frac{n_h}{n_e}\omega_p > \nu_{eff} \approx \frac{60 n_e}{T^{3/2}} \ [\text{s}^{-1}],$$

where ω_p is the plasma frequency and ν_{eff} is the effective frequency of collisions between electrons. If the observed emission is generated on the second harmonic of plasma frequency $\nu_p \approx 8.97 \times 10^3 \sqrt{n_e}$ s^{-1}, taking $\nu = 2\nu_p \approx 1.4 \times 10^{11}$ s^{-1} (140 GHz), we obtain $n_e \approx 6.4 \times 10^{13}$ cm^{-3}. Hence, the number density of accelerated electrons ($E > 100$ keV, Zaitsev, *et al.*, 2013) at the temperature $T = 2 \times 10^6$ K (Zaitsev *et al.*, 2013) is

$$n_E > \frac{n_e \nu_{eff}}{\pi \nu} \approx 20 \frac{n_e^2}{\nu T^{3/2}} \approx 2 \times 10^8 \text{ cm}^{-3}.$$

This value by two orders of magnitude greater than the number density obtained from the X-ray spectral fitting of the 5 July 2012 solar flare.

In turn, taking into account that atoms and molecules make a positive contribution to the dielectric permittivity of the medium in the partially ionized chromosphere, Fleishman and Kontar (2010) proposed another non-thermal mechanism. They assumed that Cherenkov emission generated by relativistic electrons in the chromosphere can be responsible for sub-THz emission. However, the permittivity for the **chromospheric** plasma is not known whereas the extrapolation based on the Earth's atmosphere seems to be not quite reliable (Krucker *et al.*, 2013).

3.2. Thermal component

3.2.1. Millimeter bremsstrahlung emission from the corona

To estimate the contribution of the thermal coronal plasma to the flare millimeter free-free emission we used EUV observations obtained with the Atmospheric Imaging Assembly (SDO/AIA) which is sensitive with respect to plasma temperatures $T = 0.5 - 20$ MK (Lemen *et al.*, 2012).

The brightness temperature in the case of the optically thin source can be written as (Alissandrakis *et al.*, 2013; Tsap *et al.*, 2016)

$$T_b(\nu) = \frac{1}{\nu^2} \int_{T_{min}}^{T_{max}} \frac{K\phi(T)}{\sqrt{T}} e^{-\tau_\nu} dT, \tag{9}$$

where the differential emission measure **and the optical thickness τ_ν are**

$$\phi(T) = n_e^2 \frac{dl}{dT}, \quad \tau_\nu = \int_{T_{min}}^{T_{max}} \frac{K\phi(T)}{T^{3/2}\nu^2} dT,$$

where T_{min} and T_{max} correspond to the temperature range of coronal plasma **and the coefficient**

$$K = 9.78 \times 10^{-3} \times \begin{cases} 18.2 + \ln T^{3/2} - \ln \nu, & T < 2 \times 10^5 \ K \\ 24.5 + \ln T - \ln \nu, & T > 2 \times 10^5 \ K \end{cases} \ (cgs \ units).$$

Thus, taking into account the Rayleigh-Jeans law, we can estimate the spectral flux density as

$$F_\nu = \frac{2k_B \nu^2}{c^2} T_b(\nu) \frac{S_c}{R^2}, \tag{10}$$

where k_B is the Boltzmann constant, S_c is the projected area of a coronal source and R is the Sun-Earth distance.

In order to estimate F_ν, the unsaturated SDO/AIA data were calibrated using the program *aia_prep.pro* and normalized to the exposure time from six EUV wavebands (94 Å, 131 Å, 171 Å, 193 Å, 211 Å, 335 Å). Then, the differential emission measure $\phi(T)$ for the time interval 11:43:15-11:43:27 UT was calculated from the area $S_c \approx 4 \times 10^{18}$ cm^2 **(Figure 7)** corresponding to 50% RHESSI contour (CLEAN algorithm, Hurford *et al*, 2002) in the energy range of $7-10$ keV based on the Tikhonov regularization technique (Tikhonov and Arsenin, 1979; Kontar *et al.*, 2004; Kontar *et al.*, 2005; Hannah and Kontar, 2012; Motorina *et al.*, 2012; Motorina *et al.*, 2016). Results of numerical calculations of $\phi(T)$, averaged over the source area (Figure 8), show evidence that the coronal part of the flare energy release region contains a large amount of plasma with $T = 0.5 - 3$ MK. In spite of this circumstance and sufficiently large value S_c we concluded from Equations (9) and (10) that the contribution of thermal SDO plasma to the observed millimeter emission at 93 and 140 GHz should be negligibly small **since the spectral flux density proved to be about 3 s.f.u.**

3.2.2. **Millimeter bremsstrahlung emission from the transition region**

The similar behavior of millimeter and non-thermal time profiles suggests that the corresponding source areas of millimeter and hard X-ray emissions should be comparable in the transition region/chromosphere. ▮ **Indeed, accelerated electrons and thermal fluxes caused by their thermalization should be propagated along the magnetic field lines. Thus, we can assume that the area of thermal millimeter emission in the transition region/chromosphere $S_t \sim S_X$.**

As we have shown previously (Tsap *et al.*, 2016) **millimeter emission may well be more determined by cool ($T \sim 0.1$ MK) plasma of the transition region because of the relatively low temperature ($T \sim 0.01$ MK) of the chromosphere and small optical thickness of the coronal plasma. Therefore we will not take into account contributions to the thermal millimeter emission of these regions.**

To estimate the contribution of the transition region plasma to millimeter emission the well-known formula for the brightness temperature of the homogeneous plasma source

$$T_b(\nu) = T[1 - \exp(-\tau_\nu)]. \tag{11}$$

Here (Tsap *et al.*, 2016)

$$\tau_\nu = \eta_\nu l = \frac{K n_e^2}{T^{3/2} \nu^2} l,$$

where l is the size of the source along the line-of-sight or optical depth. As a result, for the total spectral flux we obtained

$$F_\nu = \frac{2 k_B \nu^2}{c^2 R^2} T[1 - \exp(-\tau_\nu)] S_t. \tag{12}$$

The available data do not provide enough constraints to determine an unique set of parameters. As an illustration, this can be achieved for the following main parameters of the optically thick source which lead to the observed spectrum presented in Figure 9: area $S_t = 2.7 \times 10^{18}$ cm^2, geometrical depth $l = 3.2 \times 10^7$ cm, plasma temperature $T = 0.1$ MK, and number density of thermal electrons $n_e = 4.5 \times 10^{11}$ cm^{-3}.

The most interesting feature of proposed model of millimeter emission is the large S_t of the optically thick cool source. The large-scale ($\sim 60''$) thermal source with the temperature $T \sim 0.1$ MK and the number density of thermal electrons $n_e \gg 2 \times 11^{10}$ cm^{-3} was previously proposed by Trottet *et al.* (2008) to explain a gradual, long-lasting (> 30 min) component of sub-THz emission from the energetic solar flare of 28 October 2003. However, in our case the source area $S_t \gg S_X$, i.e., the millimeter and hard X-ray time profiles of emission could hardly be similar that contradicts observations. It is easy to show that for other reasonable values of l, T, and n_e the problem of large source areas S_t remains.

4. Discussion and conclusions

In this paper we show that the positive spectral slope between 93 and 140 GHz revealed with the radio telescope RT-7.5 for the 5 July 2012 solar flare can be determined by gyrosynchrotron emission in the chromosphere. The analysis is based on the suggestion about common population of low energy and high energy electrons, X-ray observations, and collisional thick target model. It seems to us, the obtained results show evidence that the effective electron acceleration **or** re-acceleration (Brown *et al.*, 2009) can occur not only in the corona but also in the chromospheric part of flare loops (Tsap and Kopylova, 2017). **Note that centimeter emission as distinguished from millimeter one is generated in the corona because of the strong absorption in the chromosphere by dense and cold thermal plasma. The spectral index of high energy electrons should be harder than the spectral index of low energy ones that agrees with the well established case of a broken-power-law electron distribution.**

The formation of the positive millimeter spectral slope through the Razin effect connected with the suppression of low frequency gyrosynchrotron emission by thermal plasma is unlikely, since the number density of electrons would exceed 10^{12} cm^{-3} in this case. In turn, the self-absorption can be significant in the millimeter wave range at magnetic fields $B > 3$ kG what are not observed with the SDO/HMI magnetograms. The screening effect caused by the filament is hardly possible too because of the strong microwave emission absorption.

Electron acceleration in the chromosphere can occur due to the flute-type instability where the most favorable conditions are created because of the curvature of magnetic field lines (Zaitsev *et al.*, 2000; Zaitsev and Stepanov, 2015). The magnetic reconnection can also play an important role (Tsap, 1998; Brown

et al., 2009). Note that electron acceleration in the chromosphere by sub-Dreicer electric fields **can be quite effective** (Tsap and Kopylova, 2017) and allows us to solve some problems associated with the small effectiveness of hard X-ray generation in the collisional thick target model (Brown *et al.*, 2009).

As it was previously shown by (Tsap *et al.*, 2016) thermal plasma of the transition region with $T \approx 0.1$ MK can be responsible for millimeter emission between 93 and 140 GHz from the 4 July 2012 event (M5.3) which occurred in the same active region. However, hard X-ray emission was quite weak and the spectral flux at 140 GHz does not exceed 40 s.f.u. The 5 July 2012 solar flare appeared to be more powerful and hard X-ray emission increased few times. This implies the non-thermal nature of millimeter emission that agrees well with some results of observations and model calculations. **Thus, mechanisms that determine millimeter emission can be different for different flare events.**

In conclusion it is worth to note that detailed calculations of radio emission in magnetic loops have not been considered in this paper (see, however, Morgachev *et al.*, 2017). **One of the reasons is associated** with a lack of the reliable models of the flare solar transition/chromospheric region. Therefore, some parameters adopted by us are quite arbitrary (Graham *et al.*, 2015). In this context, simultaneous observations of flare events with the Interface Region Imaging Spectrograph and Atacama Large Millimeter Array can be proved very useful.

References

Akabane, K., Nakajima, H., Ohki, K. Moriyama, F., Miyaji, T.: 1973, A flare-associated thermal burst in the mm-wave region. *Solar Phys.* **33**, 431.

Akhmedov, S.B., Gelfreikh, G.B., Bogod, V.M., Korzhavin, A.N.: 1982, The measurement of magnetic fields in the solar atmosphere above sunspots using gyroresonance emission. *Solar Phys.* **79**, 41.

Alissandrakis, C.E., Kochanov, A.A., Patsourakos, S., Altyntsev, A.T., Lesovoi, S.V., Lesovoya, N.N.: 2013, Microwave and EUV observations of an erupting filament and associated flare and coronal mass ejections. *Pub. Astron. Soc. Japan* **65**, S8.

Brown, J.C., Turkmani, R., Kontar, E.P., MacKinnon, A.L., Vlahos, L.: 2009, Local re-acceleration and a modified thick target model of solar flare electrons. *Astron. Astrophys.* **508**, 993.

Chertok, I.M., Fomichev, V.V., Gorgutsa, R.V., Hildebrandt, J., Krüger, A., Magun, A. et al.: 1995, Solar radio bursts with a spectral flattening at millimeter wavelengths. *Solar Phys.* **160**, 181.

Correia, E., Kaufmann, P., Magun, A.: 1994, The observed spectrum of solar burst continuum emission in the submillimeter spectral range. In Proc.IAU Symp. **154**, 125.

Fernandes, L.O.T., Kaufmann, P., Correia, E., Giménez de Castro, C.G., Kudaka, A.S., Marun, A., Pereyra, P., Raulin, J.-P., Valio, A.B.M.: 2017, Spectral trends of solar bursts at sub-THz frequencies. *Solar Phys.***292, id.21.**

Fleishman, G.D. and Kuznetsov, A.A.: 2010, Fast gyrosynchrotron codes. *Astrophys. J.***721**, 1127.

Fleishman, G.D. and Kontar, E.P.: 2010, Sub-Thz radiation mechanisms in solar flares. *Astron. Astrophys.***709**, L127.

Giménez de Castro, C.G., Trottet, G., Silva-Valio, A., Krucker, S., Costa, J.E.R., Kaufmann, P. et al.: 2009, Submillimeter and X-ray observations of an X class flare. *Astron. Astrophys.***507** 433.

Graham, D. R., Fletcher, L., Labrosse, N.: 2015, Determining energy balance in the flaring chromosphere from oxygen V line ratios. *Astron. Astrophys.***584**, id.A6.

Guidice, D. A., Cliver, E. W., Barron, W. R., Kahler, S.: 1981, The Air Force RSTN System: *In: Bulletin of the American Astronomical Society* **13**, 553.

Hannah, I.G. and Kontar, E.P.: 2012, Differential emission measures from the regularized inversion of Hinode and SDO data. *Astron. Astrophys.***539**, id.A146.

Hildebrandt, J., Krüger, A., Chertok, L.M., Fomichev, V.V., and Gorgutsa, R V: 1998, *Solar Phys.***181**, 337.

Hurford, G.J., Schmahl, E.J., Schwartz, R.A., Conway, A.J., Aschwanden, M.J., Csillaghy, A. et al.: 2002, The RHESSI Imaging Concept. *Solar Phys.***210**, 61.

Kaufmann, P., Correia, E., Costa, J.E.R. and Zodi, V.A.M.: 1986, A synchrotron/inverse Compton interpretation of a solar burst producing fast pulses at lambda less than 3-mm and hard X-rays. *Astron. Astrophys.***157**, 11.

Kaufmann, P., Raulin, J.-P., Gimenez de Castro, C.G., Levato, H., Gary, D.E., Costa, J.E. R. et al.: 2004, A new solar burst spectral component emitting only in the terahertz range. *Astrophys. J.***603**, L121.

Kaufmann, P. and Raulin, J.-P.: 2006, Can microbunch instability on solar flare accelerated electron beams account for bright broadband coherent synchrotron microwaves? *Physics of Plasma* **13**, 070701.

Kaufmann, P., Trottet, G., Gimenez de Castro, C.G. Raulin, J.-P., Krucker, S., Shih, A.Y. et al.: 2009, Subterahertz, microwaves and high energy emissions during the 6 December 2006 flare, at 18:40 UT. *Solar Phys.***255**, 131.

Kontar, E.P., Piana, M., Massone, A.M., Emslie, A.G., and Brown, J.C.: 2004, Generalized regularization techniques with constraints for the analysis of solar bremsstrahlung Xray spectra. *Solar Phys.***225**, 293.

Kontar, E. P., Emslie, A. G., Piana, M., Massone, A.M., Brown, J.C.: 2005, Determination of electron flux spectra in a solar flare with an augmented regularization method: application to Rhessi data. *Solar Phys.***226**, 317.

Krucker, S., Gimenez de Castro, C.G., Hudson, H.S., Trottet, G., Bastian, T.S., Hales, A.S. et al.: 2013, Solar flares at submillimeter wavelengths. *Astron. Astrophys. Rev.***21**, id.58.

Kundu, M.R., White, S.M., Gopalswamy, N., Lim, J.: 1994, Millimeter, microwave, hard X-ray, and soft X-ray observations of energetic electron populations in solar flares. *Astron. Astrophys. Suppl.***90**, 599.

Lemen, J.R., Title, A.M., Akin, D.J., Boerner, P.F., Chou, C., Drake, J.F. et al.: 2012, The atmospheric imaging assembly (AIA) on the solar dynamics observatory (SDO). *Solar Phys.***275**, 17.

Lin, R.P., Dennis, B.R., Hurford, G.J., Smith, D.M., Zehnder, A., Harvey, P.R. et al.: 2002, The Reuven Ramaty High-Energy Solar Spectroscopic Imager (RHESSI). *Solar Phys.***210**, 3.

Lüthi, T., Magun, A., and Miller, M.: 2004, First observation of a solar X-class flare in the submillimeter range with KOSMA. *Astron. Astrophys.***415** 113.

Machado, M. E., Avrett, E.H., Vernazza, J.E. and Noyes, R.W.: 1980, Semiempirical models of chromospheric flare regions. *Astrophys. J.***242**, 336.

Morgachev, A.S., Tsap, Y.T., Smirnova, V.V., , Motorina, G.G., Kuznetsov, S.A.: 2017, Modeling of microwave emission from magneic arc with growing spectrum. *Geomagnetism and Aeronomy* **57, 1028.**

Motorina, G.G., Koudriavtsev, I.V., Lazutkov, V.P., Matveev, G.A., Savchenko, M.I., Skorodumov, D.V., and Charikov, Yu.E.: 2012, On the reconstruction of the energy distribution of electrons accelerated in solar flares. *Tech. Phys.* **57**, 1618.

Motorina, G.G., Koudriavtsev, I.V., Lazutkov, V.P., Savchenko, M.I., Skorodumov, D.V.,and Charikov, Yu.E: 2016, Reconstruction of the energy spectrum of electrons accelerated in the April 15, 2002 solar flare based on IRIS X-ray spectrometer measurements. *Tech. Phys.* **61**, 525.

Qu, Z.–Q., Xu, Z., Key properties of solar chromospheric line formation process: 2002, *Chin. J. Astron. Astrophys.* **2**, 71.

Ramaty, R., Petrosian, V.: 1972, Free-Free absorption of gyrosynchrotron radiation in solar microwave bursts. *Astrophys. J.***178, 241.**

Ramaty, R., Schwartz, R.A., Enome S., H. Nakajima: 1994, Gamma-ray and millimeter-wave emissions from the 1991 June X-class solar ares. *Astrophys. J.***, 436, 941**

Raulin, J.-P., White, S.M., Kundu, M.R., Silva, A.V.R., Shibasaki, K.: 1999, Multiple components in the millimeter emission of a solar flare. *Astrophys. J.***522**, 547.

Raulin, J.P., Makhmutov, V.S., Kaufmann, P., Pacini, A.A., Lüthi, T., Hudson, H.S. et al.: 2004, Analysis of the impulsive phase of a solar flare at submillimeter wavelengths. *Solar Phys.***223**, 181.

Rozanov, B.A.: 1981, Millimeter range radio telescope RT-7.5 BMSTU. *In Reviews of USSR Universities, part 3, Radio electronics* **24**, 3.

Sakai, J.I., Nagasushi, Y.: 2007, Emission of electromagnetic waves by proton beams in solar plasmas. *Astron. Astrophys.***474**, 33.

Schwartz, R.A., Csillaghy, A., Tolbert, A.K., Hurford, G.J., McTiernan, J., Zarro, D.: 2002, RHESSI Data Analysis Software: Rationale and Methods. *Solar Phys.***210**, 165.

Silva, A.V.R., Share, G.H., Murphy, R.J., Costa, J.E.R., Gimenez de Castro, C.G., Raulin, J.-P. et al.: 2007, Evidence that synchrotron emission from nonthermal electrons produces the increasing submillimeter spectral component in solar flares. *Solar Phys.***245**, 311.

Smirnova, V.V., Nagnibeda, V.G., Ryzhov, V.S. Zhil'tsov, A.V., Solov'ev, A.A.: 2013, Observations of subterahertz radiation of solar flares with an RT-7.5 radiotelescope. *Geomagnetism and Aeronomy* **53**, 997.

Tikhonov, A.N., Arsenin V.Y., 1979, *Methods of solutions of ill-posed problems*, Nauka, Moscow (in Russian).

Trottet, G., Vilmer, N., Barat, C., Benz, A., Magun, A., Kuznetsov, A., Sunyaev, R., Terekhov, O.: 1998, A multiwavelength analysis of an electron-dominated gamma-ray event associated with a disk solar flare. 334, 1099.

Trottet, G., Raulin, J., Kaufmann, P., Siarkowski, M., Klein, K.-L., Gary, D.E.: 2002, First detection of the impulsive and extended phases of a solar radio burst above 200 GHz. *Astron. Astrophys.***381**, 694.

Trottet, G., Krücker, S., Lüthi, T., Magun, A.: 2008, Radio submillimeter and ?-ray observations of the 2003 October 28 solar flare. *Astrophys. J.***678**, 509.

Trottet, G., Raulin, J.-P., Giménez de Castro, G., Lüthi, T., Caspi, A., Mandrini, C.H. et al.: 2011, Origin of the submillimeter radio emission during the time-extended phase of a solar flare. *Solar Phys.***273** 339.

Tsap, Yu.T. :1998, The stochastic acceleration of upper chromospheric electrons. *Astron. Rep.* **42** 275.

Tsap, Y.T., Smirnova, V.V., Morgachev, A.S., Motorina, G.G., Kontar, E.P., Nagnibeda, V.G. et al.: 2016, On the origin of 140 GHz emission from the 4 July 2012 solar flare. *Solar Phys.***57**, 1449.

Tsap, Y.T., Kopylova Y.G.: 2017, Coulomb collisions and electron acceleration in the sub-Dreicer electric fialds of the solar corona and chromosphere. *Geomagnetism and Aeronomy* **57, 996.**

White, S.M., Kundu, M.R.: 1992, Solar observations with a millimeter-wavelength array. *Solar Phys.***141, 347.**

White, S.M., Thomas, R.J., Schwartz, R.A.: 2005, Updated expressions for determining temperatures and emission measures from GOES soft X-ray measurements. *Solar Phys.***227**, 231.

White, S.M., Benz, A.O., Christe, S., Fárnik, F., Kundu, M.R., Mann, G. et al.: 2011, The relationship between solar radio and hard X-ray emission. *Space Sci. Rev.***159**, 225.

Zaitsev, V.V., Urpo, S., Stepanov, A.V.: 2000, Temporal dynamics of Joule heating and DC-electric field acceleration in single flare loop. *Astron. Astrophys.***357**, 1105.

Zaitsev, V.V., Stepanov, A.V., Melnikov, V.F.: 2013, Sub-terahertz emission from solar flares: the plasma mechanism of chromospheric emission. *Astron. Lett.* **39**, 650.

Zaitsev, V.V., Stepanov, A.V.: 2015, Particle acceleration and plasma heating in the chromosphere. *Solar Phys.***290**, 3559.

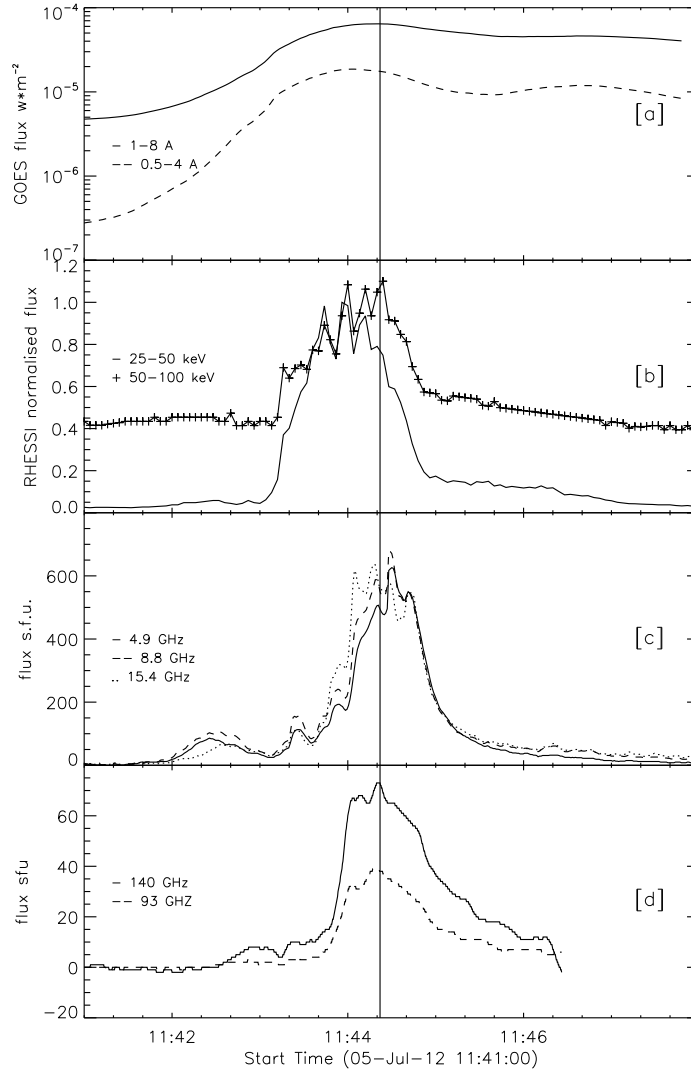Zheleznyakov, V.V.: 1970, Radio Emission of the Sun and Planets, Pergamon Press, 697.

Figure 1. Time profiles of X-ray, microwave, and millimeter emission fluxes from the 5 July 2012 solar flare obtained with GOES [a] and RHESSI [b] satellites as well as RSTN [c] (San Vito), and RT-7.5 [d] radio telescopes. The vertical solid line corresponds to the peak of millimeter emission (11:44:24 UT).
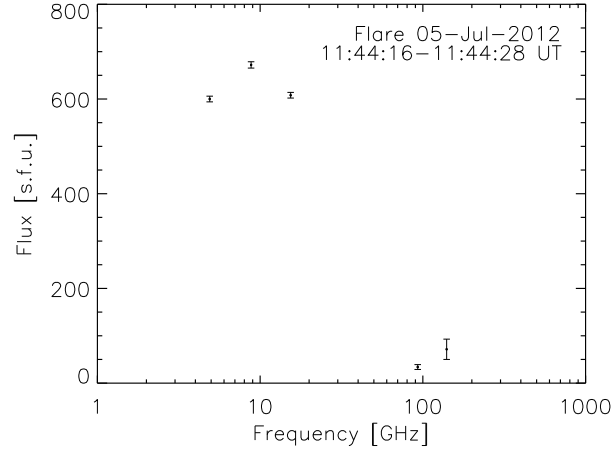
Figure 2. The averaged over the time interval (11:44:16-11:44:28 UT) radio flux density spectrum of the 5 July 2012 solar flare at frequencies 4.9, 8.8, and 15.4 GHz (RSTN, San Vito) as well as 93 and 140 GHz (RT-7.5, Bauman Moscow State Technical University).
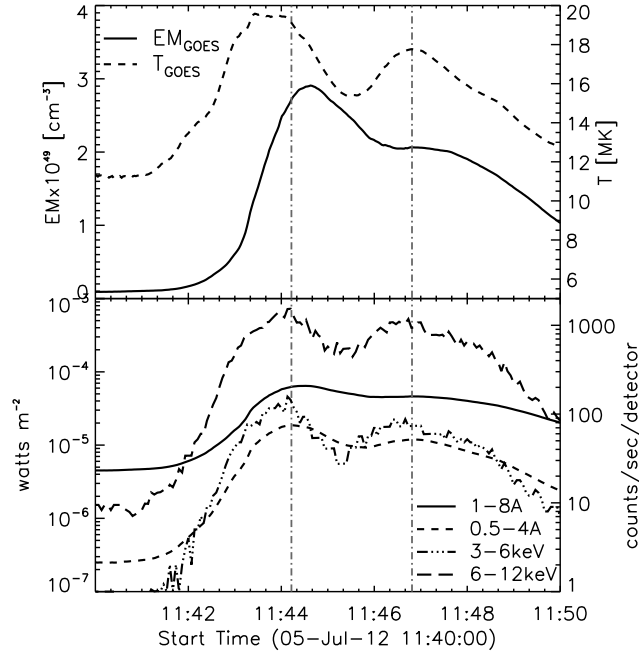
Figure 3. Upper panel: temperature and emission measure time profiles of the 5 July 2012 solar flare obtained from GOES observations (0.5-4 Å, 1-8 Å). The vertical dash-dotted lines indicate two peaks of 0.5-4 Å light curve at 11:44:13 UT and 11:46:49 UT. Lower panel: soft X-rays light curves obtained with GOES and RHESSI (3-6 keV, 6-12 keV) observations.
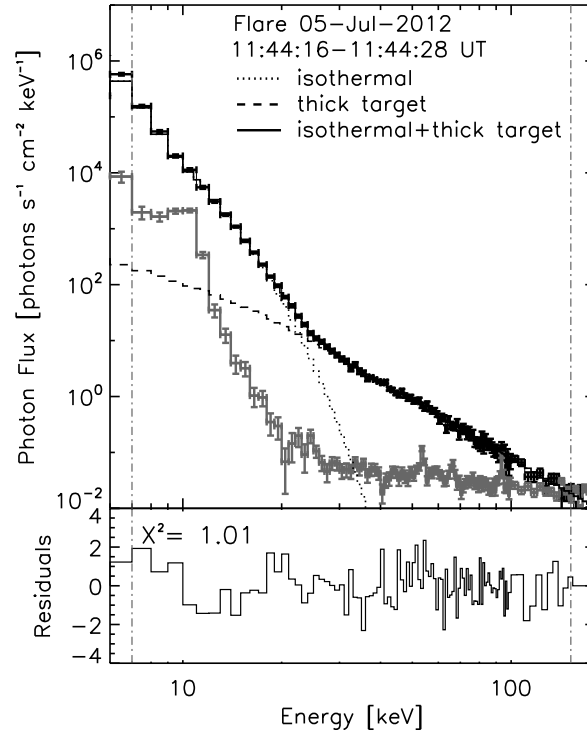
Figure 4. Upper panel: RHESSI background-subtracted photon flux spectrum (black line) with background (gray histogram) and fitted model (black histogram), which consists of isothermal (dotted histogram) and collisional thick target (dashed histogram) models. Bottom panel: the ratio of the difference between observed and fitted data to the corresponding errors for RHESSI measurements. For both panels the vertical dash-dotted lines indicate the fitted energy range $(7 - 155 \text{ keV})$.
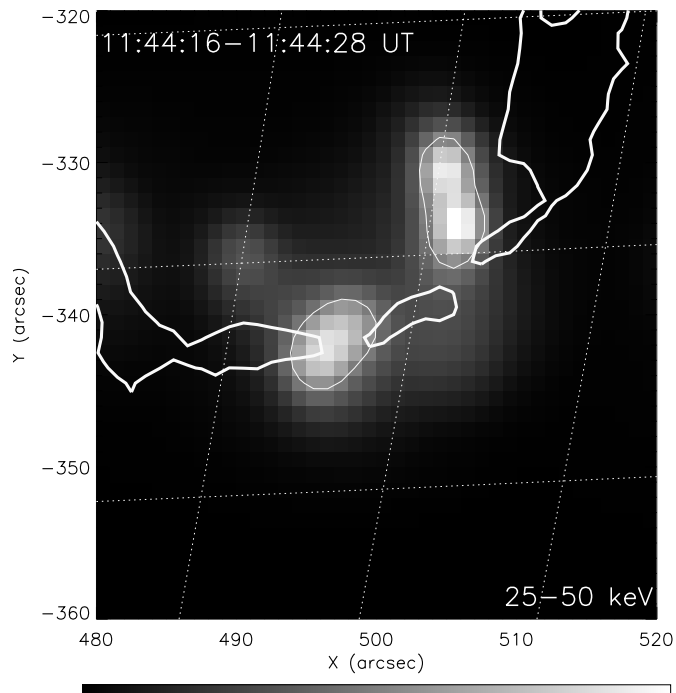
Figure 5. The hard X-ray image from 25 to 50 keV of the 5 July 2012 solar event. The contours (thin white solid curves) correspond to the 50% of the peak emission. Magnetic polarity inversion lines derived from the SDO/HMI magnetogram are shown by the thick white solid curves. The PIXON algorithm was used for the reconstruction of images.
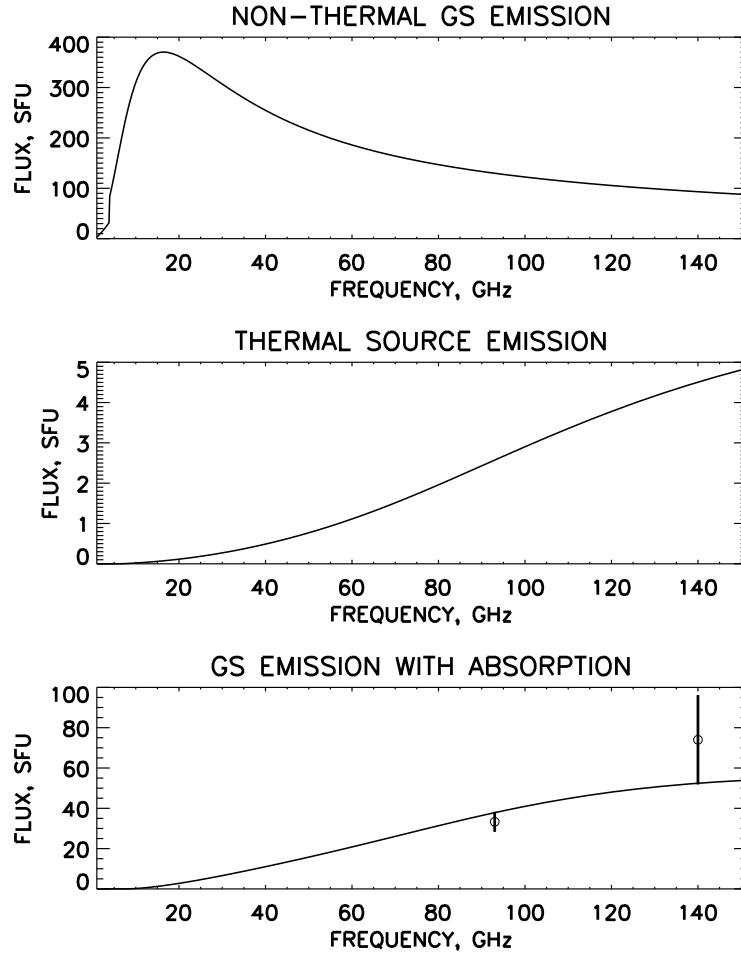
Figure 6. The numerical simulation of millimeter emission spectrum from the 5 July 2012 event in the chromosphere. Gyrosynchrotron emission of non-thermal electrons without chromospheric absorption (upper figure) and free-free emission (middle figure). Bottom figure: Observational data (circles) with error bars at 93 and 140 GHz and modelled total flux spectrum (solid line) of the chromospheric source. Parameters are described in the main text.
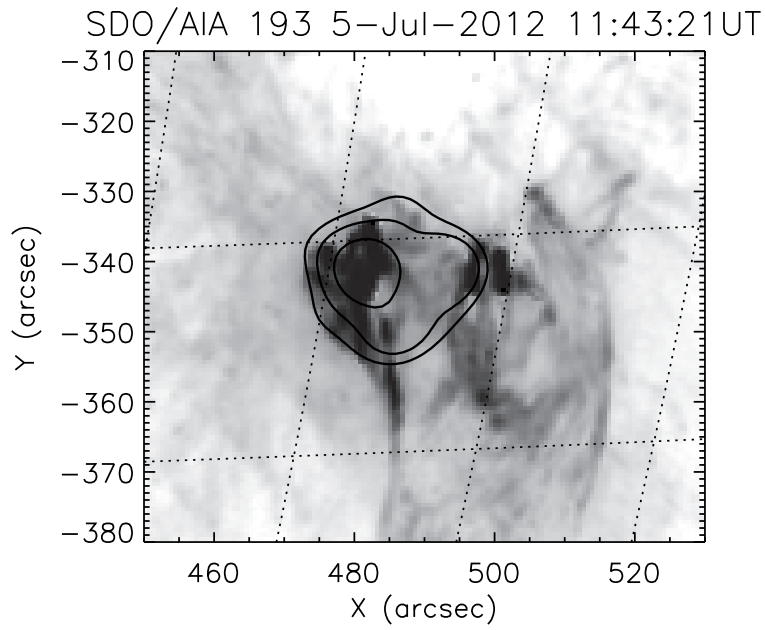
Figure 7. The AIA 131Å map overlaid with RHESSI 7-10 keV contours (11:43:00-11:43:20 UT) at 40, 50, and 70% of the peak intensity during the 5 July 2012 solar event. The CLEAN algorithm was used for the reconstruction of images.
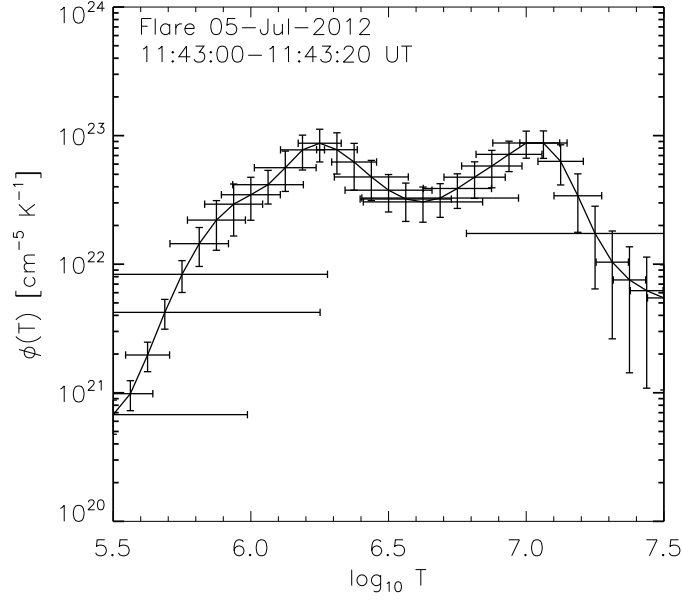
Figure 8. The regularized differential emission measure $\phi(T)$ obtained from SDO/AIA data for the 5 July 2012 solar flare. The vertical and horizontal lines correspond to $\Delta\phi(T)$ and $\Delta\lg T$, respectively.
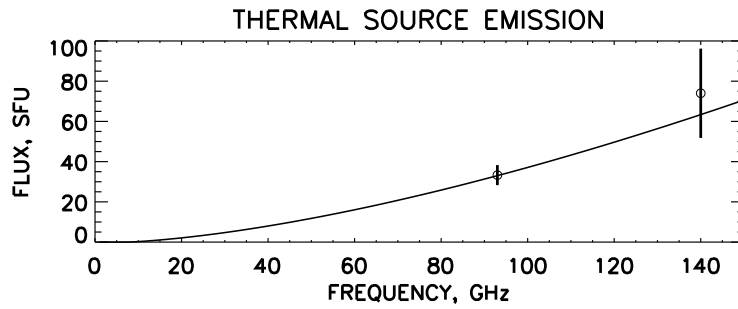

Figure 9. Results of numerical simulations of free-free emission from the 5 July 2012 solar flare (11:44:24 UT) obtained from Equation (12).